Continuous-variable entanglement distillation between remote quantum nodes

Yanhong Liu,[1] Jieli Yan,[1] Lixia Ma,[1] Zhihui Yan,[1,2,*] and Xiaojun Jia[1,2]

[1]*State Key Laboratory of Quantum Optics and Quantum Optics Devices, Institute of Opto-Electronics, Shanxi University, Taiyuan 030006, People's Republic of China*

[2]*Collaborative Innovation Center of Extreme Optics, Shanxi University, Taiyuan 030006, People's Republic of China*

(Received 2 April 2018; published 6 November 2018)

The development of quantum network relies on high-quality entanglement between remote quantum nodes. In reality the unavoidable decoherence limits the quality of entangled quantum nodes, however, entanglement distillation can overcome this problem. Here we propose an experimentally feasible scheme of continuous-variable entanglement generation, storage, and distillation between distant quantum nodes, which only requires the atomic ensemble quantum memory and balanced homodyne detection (BHD). Initially one copy of a bipartite entangled state of light, suffering phase fluctuations during the distributions, is stored in two distant atomic ensembles so that the atomic ensembles are entangled. Within the storage lifetime, by distributing and storing another copy of entangled optical modes in these two atomic ensembles, the distillation on entangled atomic spin waves can be implemented based on the post-selection of the BHD result. Our scheme provides a highly entangled state between remote quantum nodes for downstream applications, and enables the extension to multipartite entanglement distillation in a large-scale quantum network.

DOI: 10.1103/PhysRevA.98.052308

I. INTRODUCTION

In a quantum network, consisting of quantum nodes and quantum channels, stationary quantum nodes are used to store and process flying quantum information, and quantum channels play the role of transmission of quantum information and connecting quantum nodes [1]. The constructions of quantum nodes have been realized in different kinds of physical systems, such as atomic ensembles [2–9], single atoms [10–12], trapped ions [13–15], superconductors [16,17], optomechanics [18–23], solid-state systems [24–28], and so on. Particularly, atomic ensemble as one of the ideal candidates for quantum nodes has attracted extensive attention, due to the collective enhancement of light-atom interaction. On the other hand, quantum entanglement is not only a striking feature of quantum physics, but also plays a core role in fields of quantum information science, including quantum teleportation, quantum cryptography, quantum secret sharing, and quantum computation [29–32]. The quantum network will rely on the ability to generate, distribute, and store entanglement among quantum nodes [1,33], and thus the generation of high-quality entanglement between remote atomic ensembles is a long-standing goal for the development of quantum information science. The high-quality atom entanglement can be obtained based on high-efficiency quantum storage and highly squeezed optical modes. The squeezed state of 15 dB has been experimentally generated [34], and cavity enhanced light-atom interaction enables high-efficiency quantum memory [35,36]. However, the entanglement between remote quantum nodes is vulnerable to the unavoidable decoherence arising from the loss, and phase fluctuation during the entanglement distribution, which degrade the entanglement quality and limit the distance between quantum nodes. Fortunately, the quantum repeater [37,38], composed of quantum memory [39–46], entanglement distillation [47–53], and entanglement swapping [54,55], can conquer this detrimental effect.

Entanglement distillation, which can extract a small set of highly entangled states from a large supply of weakly entangled states in the presence of unavoidable decoherence, enables high-quality entanglement between remote quantum nodes in the quantum network [47,48]. For the discrete-variable (DV) quantum system, the distilled entangled photon pairs can be obtained by means of local operation and classical communication [53]. In the field of the continuous-variable (CV) regime, which paves another avenue towards the implementation of quantum information science, the information is encoded into continuous degrees of freedom of physical systems such as field modes of light or the collective atomic spin states [56–59]. Recently, the proof-of-principle experimental demonstrations of entanglement distillation on the nonclassical state of light have been successfully carried out by using measurement-induced non-Gaussian operations. For example, subtracting a single photon, yielding a non-Gaussian state from the initial Gaussian state, makes entanglement distillation come true [60,61]. With the development of quantum information, preparing of distilled entanglement between remote quantum nodes in the quantum network is the building block of various high-fidelity quantum information protocols. Besides the important application of entanglement distillation in quantum communication [38,62], it also plays a central role for quantum computation [63], because it can significantly increase the quality of logic operations between different elementary logic units. The efficient and nondestructive DV entanglement distillation with improved fidelity in atomic quantum nodes has been experimentally realized. Two pairs of

*zhyan@sxu.edu.cn

entangled ions, which are confined in a linear multizone Paul trap, are created and connected by phase gates, and measured by state-dependent fluorescence [64]. The distillation of a remote entangled state with increased fidelity for further use has been heralded by single-photon mediated entanglement of the electron spins (communication qubits), robust storage in the nuclear spins (memory qubits), and local operations. The electron spin entanglement is produced by two sets of entanglement between a photon and electron spin together with the low efficiency or complex single-photon detection [65]. For the CV quantum distillery, although it is probabilistic, the failed operation merely degrades the quality of entangled quantum nodes. Datta *et al.* have shown a CV entanglement distillation scheme consisting of four atomic ensembles to act as nonlinear and linear elements for generating, storing, and distilling entanglement, where 50% storage efficiency, near-perfect retrieval efficiency, as well as single-photon and vacuum detection are required [66]. For the future development of quantum network, it is still challenging to explore feasible preparation of the distilled CV entanglement between remote atomic ensembles for further downstream applications.

In this paper, we propose CV entanglement distillation between two remote separated atomic ensembles, which can overcome the influence of phase noise in the entanglement distribution channels. In our scheme, only one set of the entangled resource of light is employed and two atomic ensembles without the need of cooling and trapping systems can be used as the candidates of quantum nodes; besides balanced homodyne detection (BHD) with a near-perfect efficiency diode is required, instead of single-photon detection. In addition the entanglement distillery works well in a broad range of storage efficiency and is independent of retrieval efficiency. In this feasible entanglement distillation procedure, the local interference between phase-diffused entangled atomic spin waves and phase-diffused entangled optical modes at each location and post-selection are employed, which is easily implemented by only well-established Gaussian operation technology, including atomic-ensemble quantum memory and BHD. The atomic-ensemble quantum memory can provide the required storage efficiency for local interference in entanglement distillation. The post-selection is realized based on the BHD results of the optical modes emerging from atomic ensembles. Neither non-Gaussian operation and measurement nor perfect quantum state mapping efficiency is involved in our scheme, which is simple to implement in experiment. First, entangled optical modes can be produced by two degenerate optical parameter amplifiers (DOPAs) and a beam splitter, and distributed to two remote atomic ensembles. The random phase fluctuation is a natural noise source in the quantum channel, which will give rise to a non-Gaussian entangled state. Subsequently phase-diffused entangled optical modes are stored in atomic spin waves of two atomic ensembles to establish the entanglement between these atomic spin waves. The entanglement distillation begins with a non-Gaussian entangled state between two atomic spin waves. Afterwards, a fresh copy of such kinds of entangled optical modes is interfered with atomic spin waves stored in atomic ensembles. Finally, by conditioning the BHD results of the interference output fields, the successful realization of entanglement distillation of atomic spin waves can be obtained, which enables the downstream applications in quantum network, such as the highly faithful quantum information network. By applying the total variance between two atomic ensembles, we can check the entanglement distillation performance, and the dependencies of total variances on systematic parameters are theoretically investigated. The calculation results numerically demonstrate that our proposal overcomes the phase noises in the quantum channels of entangled optical modes, and improves the quality of CV atom entanglement for quantum information applications. The protocol can make it possible to regain the nonclassical property even when the atom entanglement before distillery almost disappears, and to extend the distance between quantum nodes.

The paper is organized as follows. The generation, distribution, storage, and distillation of entanglement between two space-separated quantum nodes are investigated in Sec. II. In Sec. III we will study the performance of entanglement distillation between two atomic ensembles, and analyze the experimental parameters' influence on the entanglement distillation effect. And a brief summary is provided in Sec. IV.

II. SCHEME OF GENERATION AND DISTILLATION OF ENTANGLEMENT BETWEEN QUANTUM MEMORIES

Our protocol consists of the nonclassical source for generating EPR entangled optical pulses, two atomic ensembles as quantum nodes, and two sets of BHD systems. Especially, it requires two operation procedures of storing entangled optical pulses in atomic ensembles. Due to the random phase fluctuations in entanglement distribution channels, they transform the quantum state of light from the pure Gaussian entangled state into the mixed non-Gaussian entangled state. In the first quantum memory procedure for atom entanglement establishment, two atomic ensembles are entangled by means of linearly mapping the quantum state from optical modes to atomic spin waves, and thus the atomic ensembles are also in the mixed non-Gaussian entangled state. In the second quantum memory procedure for atom entanglement distillation, quantum interference between the second entangled optical pulses and entangled atomic spin waves enables one to distill atomic spin wave entanglement, together with conditioning of the BHD measurement outcome. The entanglement distillation procedure can reduce the total variance of the mixed non-Gaussian entangled state between atomic ensembles by only retaining the results with small phase fluctuations.

The complete steps of the entanglement distillation protocol are depicted in Figs. 1(a) and 1(b). Figure 1(a) shows the process of generation and distribution of entangled optical modes. Entangled optical modes L_1^1 and L_2^1 are prepared by coupling two squeezed optical fields on a beam splitter, and then distributed to two remote atomic ensembles A_1^0 and A_2^0 through the quantum channels, where the phase diffusion noises act as the de-Gaussifying operation. The resulting two entangled optical modes L_1^1 and L_2^1 are stored in two atomic ensembles A_1^0 and A_2^0, so that these two atomic spin waves after quantum storage A_1^1 and A_2^1 are in an entangled state, as a result of linear mapping of quantum states from input entangled optical modes into atomic spin waves. Figure 1(b) depicts the process of distillation of entangled atomic ensembles. Another copy of entangled optical modes is generated,

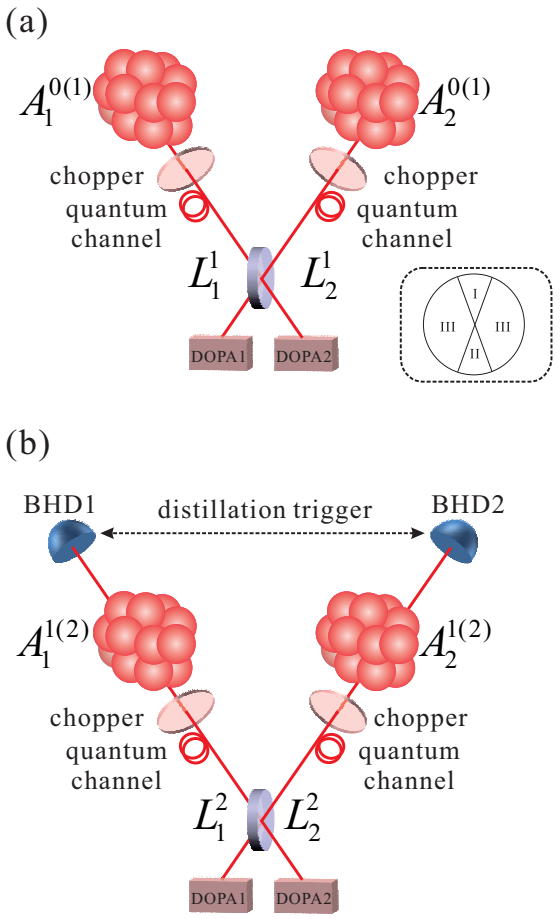

FIG. 1. Schematic of entanglement distillation between two distant atomic ensembles. (a) Generation and distribution of one copy of entangled optical modes to two remote atomic ensembles. $A_1^{0(1)}$ and $A_2^{0(1)}$ are atomic ensembles before (after) the first quantum storage. (b) Entanglement distillation by means of storing another copy of entangled optical modes in these two atomic ensembles, and BHD based post-selection. A_1^2 and A_2^2 are atomic ensembles after entanglement distillery. The insert is the structure of the optical chopper.

distributed, and stored in these two atomic ensembles, which allow the local interference between the input entangled optical modes L_1^2 and L_2^2 and the entangled atomic spin waves after quantum storage A_1^1 and A_2^1 in linear beam-splitter-type quantum memories. Afterwards, the transmitted optical modes from two atomic ensembles are measured by two sets of BHDs, and the successful measurement results herald the highly entangled atomic spin waves after distillation A_1^2 and A_2^2 are obtained, which can be used for further quantum information applications. In the atom entanglement distillation protocol, the two input parts of the interference usually have the same quantum correlation degree [49,67]. The structure of the optical chopper, shown in the insert of Fig. 1, is employed in our protocol, and two slits are carved in the disk. In zone I, nothing is in the slit; in zone II, an attenuator is attached here; in zone III, it is made of metal material to block the optical beams. In Fig. 1(a) (zone I of the optical chopper works), the optical modes pass the choppers without attenuation for the first quantum memory. In Fig. 1(b) (zone II of the optical chopper works), the optical modes pass the choppers with a variable transmissivity, so that this operation provides optical modes with a desirable quantum correlation degree for the second quantum memory. The EIT process is used as a beam splitter to realize the interference between the second copy of entangled optical modes and atomic spin waves in two atomic ensembles, which are entangled as a result of quantum state mapping from the first copy of entangled optical modes. The quantum correlation degree between atomic spin waves is worse than that between the second copy of optical modes, because of the limited storage efficiency, so two choppers are introduced to attenuate the quantum correlation degree of the optical modes in the second round, and thus the quantum correlation degree of the second optical fields is equal to that of the atomic ensembles, which is similar to previous schemes [49,67]. And thus the transmissivity of the chopper is chosen as the same value of storage efficiency of the atomic ensemble, which is equal in the first and second rounds. Finally when zone III of the optical chopper works, the optical modes are blocked, so the BHD outputs the quantum noise limit (QNL). Therefore the optical pulses after the entanglement distribution always remain the mixed non-Gaussian state with (zone I) and without (zone II) the attenuation because the attenuation plays the role of the linear beam splitter.

The inseparability criterion can be applied in verifying EPR entanglement, and in the criterion the quantum correlation of the Gaussian state can be quantified by the total variance $\Delta\mathrm{EPR} = \langle(\delta\hat{x})^2\rangle + \langle(\delta\hat{p})^2\rangle$, which is the sum of correlation variances of quadrature amplitudes and quadrature phases [68,69]. If the total variance ΔEPR is less than QNL as $\Delta\mathrm{EPR} < 1$, then the state is entangled. In the first and second quantum memory procedures, two atomic ensembles are in the mixed non-Gaussian entangled state, as a result of the phase noises in entanglement distribution channels. Although for the mixed non-Gaussian state, the total variance is strictly speaking not an entanglement measurement, it can be used to quantify the degree of quantum correlations between two quantum systems and is able to be easily observed by using BHD in the experiment [49,70]. The performances of quantum entanglement between two atomic spin waves before and after entanglement distillation can be verified by the total variances.

First of all, the production of entangled optical modes is required for both atom entanglement generation and distillation. The generation of the Einstein-Podolsky-Rosen (EPR) entangled state of light can be realized by interference of the quadrature amplitude squeezed state and the quadrature phase squeezed state on the 50:50 beam splitter. Parametric down-conversion is one of the well-established techniques for generation of the nonclassical state of light [71,72]. The DOPA1 and DOPA2 operate in parametric de-amplification and amplification to produce quadrature amplitude and phase squeezed states of light, respectively, and then are coupled on the beam splitter with 0 relative phase. The output optical modes form the EPR entangled state, and they are chopped into optical pulses which can interact with atomic spin waves. The initial quantum state from the output of beam splitter interference between output squeezed states of two DOPAs is the pure Gaussian EPR entangled state. And the Wigner

function of the coupled mode $\hat{x}^1_{L,\pm} = (\hat{x}_{L^1_1} \pm \hat{x}_{L^1_2})/\sqrt{2}$ and $\hat{p}^1_{L,\pm} = (\hat{p}_{L^1_1} \pm \hat{p}_{L^1_2})/\sqrt{2}$ of the first copy of entangled optical modes L^1_1 and L^1_2 is

$$W = \frac{1}{4\pi^2 V_S^L V_{\rm AS}^L} \times \exp\left[-\frac{\left(\hat{x}^1_{L,-}\right)^2}{2V_S^L} - \frac{\left(\hat{x}^1_{L,+}\right)^2}{2V_{\rm AS}^L}\right] \times \exp\left[-\frac{\left(\hat{p}^1_{L,-}\right)^2}{2V_{\rm AS}^L} - \frac{\left(\hat{p}^1_{L,+}\right)^2}{2V_S^L}\right], \quad (1)$$

where $V_S^L = e^{-2r}/2$ and $V_{\rm AS}^L = e^{2r}/2$ are variances of the squeezing and antisqueezing components, respectively, where r is the squeezing parameter of DOPA. And the corresponding total variance is $\Delta_L^G = e^{-2r}$.

The resulting entangled optical modes are distributed to two spatially separated atomic ensembles, through the quantum channels, which will suffer the random phase fluctuations in the quantum channels. And thus the Wigner function after entanglement distribution will evolve into a positive and non-Gaussian mixed state, given by

$$W' = \frac{1}{4\pi^2 V_S^L V_{\rm AS}^L} * \int_{-\infty}^{\infty} \exp\left[-\frac{\left(\hat{x}^1_{L,-}\right)^2_\phi}{2V_S^L} - \frac{\left(\hat{x}^1_{L,+}\right)^2_\phi}{2V_{\rm AS}^L}\right] * \left[-\frac{\left(\hat{p}^1_{L,-}\right)^2_\phi}{2V_{AS}^L} - \frac{\left(\hat{p}^1_{L,+}\right)^2_\phi}{2V_S^L}\right] \Phi(\phi) d\phi, \quad (2)$$

where $(\hat{x}^1_{L,\pm})_\phi = \hat{x}^1_{L,\pm}\cos(\phi) + \hat{p}^1_{L,\pm}\sin(\phi)$, $(\hat{p}^1_{L,\pm})_\phi = \hat{p}^1_{L,\pm}\cos(\phi) - \hat{x}^1_{L,\pm}\sin(\phi)$, where $\phi = \phi_{L1} + \phi_{L2}$. $\Phi(\phi)$ is the probability distribution of the random phase fluctuation, and is assumed to exhibit Gaussian distribution with the mean zero and variance σ^2, as $\Phi(\phi) = \exp(-\phi^2/2\sigma^2)/\sqrt{2\pi\sigma^2}$. After the entanglement distribution, the total variance becomes $\Delta_L^{\rm NG} = \int_\phi (e^{-2r}\cos^2(\phi) + e^{2r}\sin^2(\phi))\Phi(\phi)d\phi$.

Electromagnetically-induced-transparency (EIT) quantum memory has the capability of capturing, storing and releasing a fast flying nonclassical state with the stationary matter system on demand. An atom with Λ type three energy level structure of a ground state $|g\rangle$, a metastable state $|m\rangle$, and an excited state $|e\rangle$ is used as the quantum memory medium [33]. The signal field corresponds to the transition between a ground state $|g\rangle$ and an excited state $|e\rangle$, while the control field is at a different wavelength of near resonance with the transition between a metastable state $|m\rangle$ and an excited state $|e\rangle$. Similarly the collective atomic spin wave is described by Stokes operator $\hat{S} = \sum |g\rangle\langle m|$, and the amplitude and phase quadratures $\hat{x}_A$ and $\hat{p}_A$ of the atom are $\hat{x}_A = (\hat{S} + \hat{S}^+)/\sqrt{2}$, $\hat{p}_A = (\hat{S} - \hat{S}^+)/\sqrt{2}i$ [59]. In our system, the control field is treated as a classical field because it is much stronger than the signal field. In a rotating frame resonant with the input carrier frequency of the quantum signal, the effective Hamiltonian $\hat{H}_{\rm EIT}$ is $\hat{H}_{\rm EIT} = i\hbar g\hat{a}\hat{S}^\dagger - i\hbar g\hat{S}\hat{a}^\dagger$ [73]. Here the effective light-atom interaction constant $g = \sqrt{N_a}\mu\Omega/\Delta$, where N_a is the number of atoms, μ is the light-atom coupling coefficient, Ω is the Rabi frequency of control field, and Δ is detuning of light and atom coupling [38,73]. According to the Heisenberg motion equation $i\hbar\frac{d}{dt}\hat{O}_i(t) = [\hat{O}_i(t), \hat{H}_{\rm EIT}]$, we can get the dynamic equation of operators for the EIT quantum memory. Under the interaction of control fields, the quantum states of the signal light and the atomic spin waves can be converted to each other. The decoherence is unavoidable in the atomic ensembles, and limits the storage lifetime. The three stages of the quantum memory process are writing, storage, and retrieval. (i) In the writing process, both the weak signal pulse and strong control field interact with an atomic medium, so that the atomic medium becomes transparent for the signal pulse and the group velocity for the signal field is reduced. As the whole signal pulse is totally compressed in the atomic medium, the control field is adiabatically switched off, the writing process occurs, and the quantum state is transferred from light into the atomic spin wave. (ii) In the storage process, the decoherence is unavoidable in the atomic medium, which limits the storage lifetime. (iii) In the retrieval process, by adiabatically switching on the control field again, the reading process happens and the quantum state can be transferred back from the atomic spin wave to the released optical mode. By solving the Heisenberg equations of the light and atomic spin wave, we obtain the solutions as follows:

$$\hat{S}(t) = \sqrt{\eta_S}\hat{a} + \sqrt{1-\eta_S}\hat{S}, \quad (3)$$

$$\hat{a}(t) = -\sqrt{\eta_R}\hat{S} + \hat{a}\sqrt{1-\eta_R}, \quad (4)$$

where both the writing efficiency η_S of quantum state transfer from the optical mode to atomic spin wave and the decoherence are considered in the storage efficiency η_S as $\eta_S = \eta_M e^{-t/\tau}$, where τ is the storage lifetime limited by atomic decoherence and η_R is retrieval efficiency. And thus quantum state mapping makes it possible to entangle quantum nodes. The required storage efficiency for local interference can be obtained by changing the control field power. Therefore, the spin waves in two atomic ensembles are entangled by high-efficiency linear mapping of the quantum state from entangled optical modes into atomic spin waves.

In the first quantum memory procedure, two atomic ensembles can be entangled by storing the entangled state of the first optical pulses in atomic spin waves. The quadrature amplitude and phase components of the coupled atomic spin waves before (after) the first quantum storage $A_1^{0(1)}$ and $A_2^{0(1)}$ are denoted as $\hat{x}^{0(1)}_{A,-} = (\hat{x}_{A_1^{0(1)}} - \hat{x}_{A_2^{0(1)}})/\sqrt{2}$, $\hat{p}^{0(1)}_{A,+} = (\hat{p}_{A_1^{0(1)}} + \hat{p}_{A_2^{0(1)}})/\sqrt{2}$. The EIT-based quantum memory process is usually treated as beam splitter interaction, and the quantum memory for the first entangled optical modes is $\hat{a}^1_{A,-} = \sqrt{\eta_S}\hat{a}^1_{L,-} + \sqrt{1-\eta_S}\hat{a}^0_{A,-}$, $\hat{a}^{1'}_{L,-} = \sqrt{1-\eta_S}\hat{a}^1_{L,-} - \sqrt{\eta_S}\hat{a}^0_{A,-}$. And thus the total variance of the mixed non-Gaussian state between atomic ensembles A_1^1 and A_2^1 is $\Delta_A^{in} = \eta_S\int_\phi(e^{-2r}\cos^2(\phi) + e^{2r}\sin^2(\phi))\Phi(\phi)d\phi + (1-\eta_S)$.

In the second quantum memory procedure, the second entangled optical pulses L_1^2 and L_2^2 will go through optical choppers, and then are stored in these two atomic ensembles A_1^1 and A_2^1 to realize the interference between the second entangled optical pulses and entangled atomic spin waves.

The second quantum memory for the quadrature amplitude is $\hat{x}^2_{A,-} = \sqrt{\eta_S}\hat{x}^2_{L,-} + \sqrt{1-\eta_S}\hat{x}^1_{A,-}$, $\hat{x}^{2'}_{L,-} = \sqrt{1-\eta_S}\hat{x}^2_{L,-} - \sqrt{\eta_S}\hat{x}^1_{A,-}$. Before light-atom interference the coupled-mode quadrature amplitude initial joint probability of the coupled mode of the first stored atomic spin waves $\hat{x}^1_{A,-}$ and the second copy of entangled optical modes $\hat{x}^2_{L,-} = (\hat{x}_{L_1^2} - \hat{x}_{L_2^2})/\sqrt{2}$ can be expressed as

$$P\left(\hat{x}^1_{A,-}, \hat{x}^2_{L,-}\right) = \frac{1}{2\pi\sqrt{V_1 V_2}} \exp\left[-\frac{\left(\hat{x}^2_{L,-}\right)^2}{2V_1} - \frac{\left(\hat{x}^1_{A,-}\right)^2}{2V_2}\right], \tag{5}$$

where $V_1 = \eta_T(V_S^L \cos^2(\phi_1) + V_{AS}^L \sin^2(\phi_1)) + (1-\eta_T)/2$, $V_2 = \eta_S(V_S^L \cos^2(\phi_2) + V_{AS}^L \sin^2(\phi_2)) + (1-\eta_S)/2$, where η_T is transmissivity of optical chopper. After quantum memory, the coupled-mode quadrature amplitude joint probability of the second stored atomic spin waves $\hat{x}^2_{A,-} = (\hat{x}_{A_1^2} - \hat{x}_{A_2^2})/\sqrt{2}$ and transmitted optical mode $\hat{x}^{2'}_{L,-} = (\hat{x}'_{L_1^2} - \hat{x}'_{L_2^2})/\sqrt{2}$ is

$$\tilde{P}\left(\hat{x}^2_{A,-}, \hat{x}^{2'}_{L,-}\right) = \frac{1}{2\pi\sqrt{A^2 - B^2}} \times \exp\left[-\frac{K\left(\hat{x}^2_{A,-}\right)^2 + M\left(\hat{x}^{2'}_{L,-}\right)^2 - N\hat{x}^2_{A,-}\hat{x}^{2'}_{L,-}}{2(A^2 - B^2)}\right], \tag{6}$$

where $A = (V_1 + V_2)/2$, $B = (V_2 - V_1)/2$, $K = 2\eta_S B + A - B$, $M = A + B - 2\eta_S B$, $N = -4B\sqrt{\eta_S(1-\eta_S)}$.

Finally, Alice and Bob measure the transmitted optical mode $\hat{X}_{\mathrm{BHD}_{1(2)}}$ by $\mathrm{BHD}_{1(2)}$, and exchange the measured results via classical communication channels, which can determine the success or failure of entanglement distillation. The distillation scheme is probabilistic operation which succeeds if the measured trigger value falls below the triggered threshold, as $\delta\hat{x} = |(\hat{x}_{\mathrm{BHD}_1} - \hat{x}_{\mathrm{BHD}_2})/\sqrt{2}| < Q$, where Q is a certain threshold to vary the selectivity of the protocol. With the help of entanglement distillation, the entanglement between final atomic ensembles A_1^2 and A_2^2 can be improved compared to that between initial atomic ensembles A_1^1 and A_2^1. And we can obtain the quadrature amplitude variance of the mixed non-Gaussian state between atomic spin waves after entanglement distillation $\langle(\delta(\hat{x}^2_{A,-}))^2\rangle$ and the success probability of entanglement distillation P as

$$\begin{aligned}\left\langle\left(\delta\left(\hat{x}^2_{A,-}\right)\right)^2\right\rangle &= \frac{1}{P}\int\int\int_{-\infty}^{\infty}\left(\hat{x}^2_{A,-}\right)^2 P_{\mathrm{cond}}\left(\hat{x}^2_{A,-}\right) \\ &\quad\times d\hat{x}^2_{A,-}\Phi(\phi_1)\Phi(\phi_2)d\phi_1 d\phi_2 \\ &= \frac{1}{P}\int\int\left[K\,\mathrm{erf}\left(\frac{Q}{\sqrt{2K}}\right) - \frac{N^2 Q}{\sqrt{8\pi}M^{3/2}}e^{-\frac{Q^2}{2M}}\right] \\ &\quad\times\Phi(\phi_1)\Phi(\phi_2)d\phi_1 d\phi_2, \end{aligned} \tag{7}$$

$$\begin{aligned} P &= \int\int\int_{-\infty}^{\infty} P_{\mathrm{cond}}\left(\hat{x}^2_{A,-}\right)d\hat{x}^2_{A,-}\Phi(\phi_1)\Phi(\phi_2)d\phi_1 d\phi_2 \\ &= \int\int \mathrm{erf}\left(\frac{Q}{\sqrt{2K}}\right)\Phi(\phi_1)\Phi(\phi_2)d\phi_1 d\phi_2, \end{aligned} \tag{8}$$

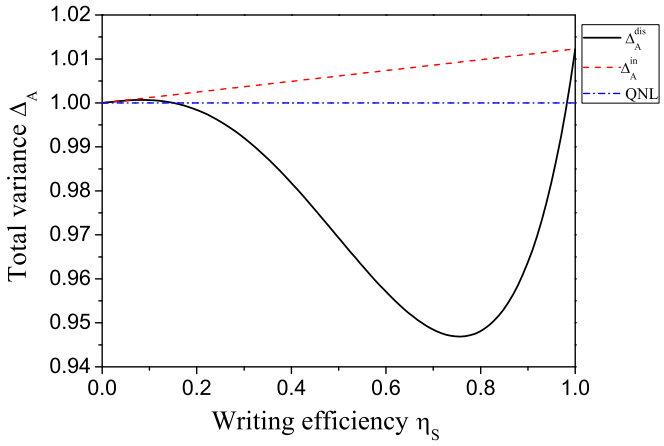

FIG. 2. The dependence of total variance Δ_A on the storage efficiency η_S. The dash-dot line is QNL. The solid line Δ_A^{dis} corresponds to the case with entanglement distillation, and the dashed line Δ_A^{in} is for the case without entanglement distillation.

where $P_{\mathrm{cond}}(\hat{x}^2_{A,-}) = \int_{-Q}^{Q}\tilde{P}(\hat{x}^2_{A,-}, \hat{x}^{2'}_{L,-})d\hat{x}^{2'}_{L,-}$ represents the unnormalized probability of the $\hat{x}^2_{A,-}$ conditional on $\delta\hat{x} < Q$.

In the following, the coupled-mode quadrature phase of the second stored atomic spin waves $\hat{p}^2_{A,+} = (\hat{p}_{A_1^2} + \hat{p}_{A_2^2})/\sqrt{2}$ is considered. When the trigger condition is satisfied, the $\langle(\delta(\hat{p}^2_{A,+}))^2\rangle$ can be reduced after entanglement distillation with the same successful probability P for $\hat{x}^2_{A,-}$, and the quadrature phase variance of the mixed non-Gaussian state between atomic spin waves after entanglement distillation $\langle(\delta(\hat{p}^2_{A,+}))^2\rangle$ is

$$\left\langle\left(\delta\left(\hat{p}^2_{A,+}\right)\right)^2\right\rangle = \frac{1}{P}\int\int K\,\mathrm{erf}\left(\frac{Q}{\sqrt{2K}}\right)\Phi(\phi_1)\Phi(\phi_2)d\phi_1 d\phi_2. \tag{9}$$

The function $\mathrm{erf}(\frac{Q}{\sqrt{2K}})$ plays the role of the filter suppressing large phase noise, and both $\langle(\delta(\hat{x}^2_{A,-}))^2\rangle$ and $\langle(\delta(\hat{p}^2_{A,+}))^2\rangle$ are reduced in this protocol. Once the trigger condition is satisfied, the quantum state shared by two atomic spin waves is projected into the higher quantum correlation state. And thus the total variance of the distilled entangled atomic spin state between two atomic ensembles $\Delta_A^{\mathrm{dis}} = \langle(\delta(\hat{x}^2_{A,-}))^2\rangle + \langle(\delta(\hat{p}^2_{A,+}))^2\rangle$ can be reduced.

III. PERFORMANCE OF ENTANGLEMENT DISTILLATION BETWEEN ATOMIC ENSEMBLES

The total variances of atomic spin waves before and after entanglement distillation are shown in Figs. 2–4, which are obtained before reading out the spin waves into optical modes. In order to verify the performance of entanglement distillery, the atomic entangled state can be converted into released optical modes in the retrieval process and measured by BHDs.

Figure 2 demonstrates the dependence of the total variance Δ_A for original and distilled atomic spin states on the storage efficiency. All parameter values are experimentally reachable to provide direct references for experimental system design. In the generation of squeezing of light at 795 nm [74], the squeezed state of light with squeezing parameter $r = 0.64$ for the rubidium atom D1 absorption line has been generated,

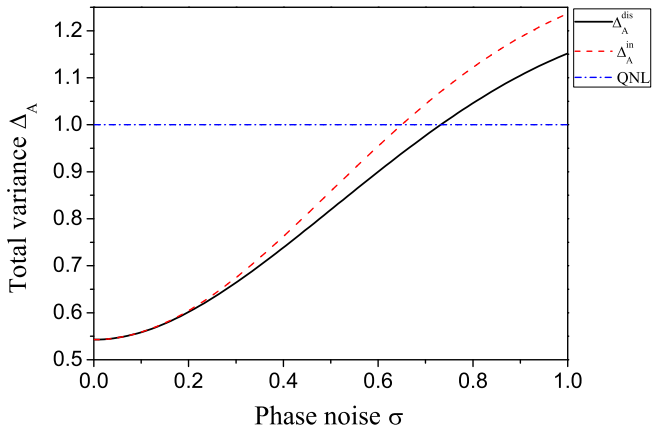

FIG. 3. The total variance Δ_A versus the phase noise. The dash-dot line is QNL. The solid (dashed) line corresponds to the case with (without) entanglement distillation.

where the corresponding squeezed degree is −5.6 dB. In the experimental work [33], the storage efficiency is usually about 48%. If the optical cavity is employed to enhance the light-matter interaction, the retrieval efficiency can reach 73% [35]. A storage-retrieval efficiency of 92% can be realized in the cold atomic media with high optical depth [75]. In our system, the experimental parameters are taken into account in the calculation as following: squeezing parameter of DOPA is $r = 0.46$, the phase diffusion noise is $\sigma = 0.66$, and certain trigger threshold is $Q = 0.45$. The dash-dot line is QNL. The solid line corresponds to the case with entanglement distillation, and meanwhile the dashed line is for the case without entanglement distillation. The smaller Δ_A is, the better the atom entanglement is. When the storage efficiency is 0 the total variance $\Delta_A^{\rm dis}$ corresponds to QNL, because no entangled optical modes are stored in atomic ensembles and the vacuum fluctuations in atomic spin waves appear. The input optical modes are totally stored with the storage efficiency of 1. In this case, no entanglement distillation occurs and atomic total variance is the phase-diffused entangled state, which is higher than the QNL. The solid line and dashed lines are overlapped at these two points, which shows that no entanglement distillation occurs. When the storage efficiency is around 0.76, the total variance $\Delta_A^{\rm dis}$ almost reaches the minimum value, and the best entanglement distillation can be obtained. For storage efficiency $\eta_S = 0.76$, the total variance $\Delta_A^{\rm dis}$ can be reduced from 1.01 to 0.95, which is better than the results with other storage efficiencies. Thus atom entanglement can be regained from the phase-diffused entangled state with the help of entanglement distillation.

Figure 3 shows the total variances Δ_A of the distilled state (solid line) and the phase-diffused state (dashed line) versus phase noise σ. All other parameter values are the same as those in Fig. 2 except the storage efficiency η_S is 0.76. The dash-dot line is QNL. The total variance of the distilled entangled state is compared with that of the phase-diffused state before distillation to quantify how effective the distillation protocol performs. We can see that the distillation protocol reduces the total variances Δ_A of the phase-diffused entangled state. The phase noise will destroy the entangled degree, and

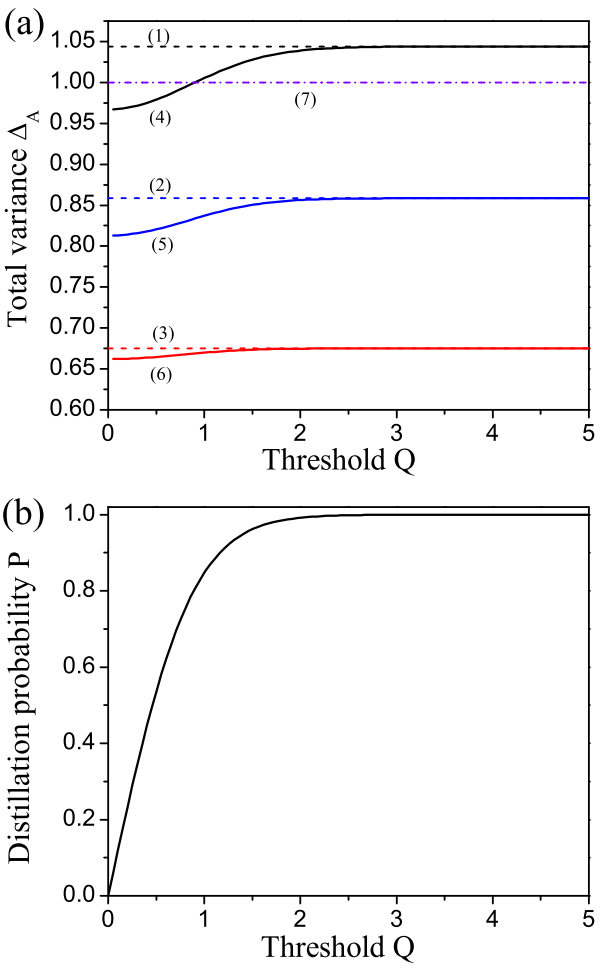

FIG. 4. (a) The function of total variance Δ_A on the threshold Q for different phase diffusion noise. Curves (1), (2), and (3) depict the total variances before distillation with phase diffusions $\sigma = 0.7$, $\sigma = 0.5$, and $\sigma = 0.3$, respectively; curves (4), (5), and (6) depict the total variances after distillation with phase diffusions $\sigma = 0.7$, $\sigma = 0.5$, and $\sigma = 0.3$, respectively; curve (7) shows QNL. (b) Distillation probability P versus the threshold Q.

even atom entanglement will disappear when the phase noise is large. However, the larger the phase noise is, the better the performance distillation protocol works. When no phase noise is introduced $\sigma = 0$, the entanglement distillation does not occur, which satisfies the no-go theorem [76]. The distillation becomes efficient for larger values of phase noise. Without entanglement distillation the entanglement is completely lost for larger levels of phase noise. For the phase diffusion noise $\sigma = 0.66$, the total variance Δ_A^{in} is larger than 1 for the initial state, which shows no nonclassical behavior. But entanglement distillation can make the total variance $\Delta_A^{\rm dis}$ below the unity boundary. The entanglement distillation protocol still can decrease the total variance from 1.01 to 0.95.

The function of total variance Δ_A for atomic ensembles and distillation probability P on the threshold Q are illustrated in Figs. 4(a) and 4(b), respectively. In Fig. 4(a), curves (1), (2), and (3) depict the total variances before distillation with phase diffusions $\sigma = 0.7$, $\sigma = 0.5$, and $\sigma = 0.3$, respectively; curves (4), (5), and (6) depict the total variances after

distillation with phase diffusions $\sigma = 0.7$, $\sigma = 0.5$, and $\sigma = 0.3$, respectively; and curve (7) shows QNL. All other parameter values are the same as those in Fig. 3. The threshold Q influences the performance of atom entanglement distillation. A trigger signal obtained as a measured quadrature value is below the chosen threshold, and its corresponding probability of successful preparation of the highly entangled state is P. If Q is close to zero, the random phase fluctuation, which mixes the noisy two-mode antisqueezed quadrature into the coupled-mode squeezing quadrature, is small. This condition selects the fraction of small phase fluctuation. For the phase diffusion noise $\sigma = 0.7$, the total variance of atomic spin waves is higher than QNL, and it is distilled to a value below QNL with the trigger threshold $Q = 0.82$. Although the big phase noise makes the total variance high, the performance of entanglement distillation is good, which can overcome the phase-diffused entangled state. This scheme is suitable for the entanglement distillery with the large phase noises. For a threshold of 0.45, a success rate is 0.5, and the distillation deploys its nearly full potential. Lower values of Q result in a stronger distillation effect but also in a reduced success probability. It is promising to find that for a success rate as high as 0.5 the protocol has nearly developed its full potential.

The phase noises are unavoidable in the entanglement distribution channels and transform the pure Gaussian entangled state into the mixed non-Gaussian state with a reduction of entanglement. When our systematic parameters are taken into account as the squeezing parameter of DOPA $r = 0.46$, random phase fluctuations in entanglement distribution channels $\sigma = 0.66$, and the storage efficiency $\eta_S = 0.76$, the total variance of the pure Gaussian entangled state of light before entanglement distribution is $\Delta_L^G = 0.4$, and the total variance of the mixed non-Gaussian state of light after the entanglement distribution is $\Delta_L^{\mathrm{NG}} = 1.012$, which is caused by the phase noises in entanglement distribution channels. And the entangled optical modes are the essential tools to entangle two atomic ensembles by means of linearly mapping the entangled state from optical modes to atomic spin waves. If the transmission distance is short or there are no phase noises in entanglement distribution channels, the two atomic ensembles are in the Gaussian entangled state, and the total variance between atomic spin waves without phase noise is $\Delta_A^G = 0.54$. However, the phase noise is inevitable, and these atomic ensembles are in the mixed non-Gaussian state, and the total variance between atomic spin waves with phase noise is $\Delta_A^{in} = 1.009$. Our atom entanglement distillation can overcome the phase noises in distribution channels, and selects the mixed non-Gaussian atom entanglement state with the small phase fluctuations to reduce the total variance. As long as the entanglement distillation between two atomic ensembles A_1^2 and A_2^2 is heralded, the quantum correlation degree between atomic spin waves is better than that of initial atomic ensembles A_1^1 and A_2^1 without entanglement distillation in the broad parametric range. Especially the quantum correlation degree between atomic spin waves can be improved to $\Delta_A^{\mathrm{dis}} = 0.95$, and the entanglement that is lost due to the phase noise in quantum channels is able to be recovered, when the proper storage efficiency is employed in entanglement distillation.

IV. SUMMARY

We have shown the feasible scheme of generation, storage, and distillation of the entangled state between remote atomic ensembles in the quantum network. In our protocol, each quantum node can be used for not only storing the quantum state but also distilling entanglement, and the atomic-ensemble quantum memory and BHD technique are involved in the quantum node. The entanglement distillation between atomic ensembles can improve the quality of the phase-diffused entangled state, which can be applied in long distance quantum communication in a wide range of physical systems, and even can regain the disappeared entanglement between long distance quantum nodes. The combination with a de-Gaussifying operation, such as single-photon substraction, would provide a CV entanglement distillation scheme capable of suppressing the effect of losses. Furthermore, the iterative entanglement distillation can provide better performance. Moreover, our scheme can be extended to other quantum information candidates, such as trapped ions, superconductors, and so on. The technique of constructing entanglement among three atomic ensembles based on entanglement mapping is compatible with our scheme, and thus makes it possible to distill multipartite entanglement in the extending network by adding more atomic ensembles and entangled optical modes. It points the way towards implementation of large-scale quantum information architecture to bridge the gap between in-principle and real-world quantum information science applications.

ACKNOWLEDGMENTS

This research was supported by the Key Project of the National Key R&D program of China (Grant No. 2016YFA0301402), the National Natural Science Foundation of China (Grants No. 61775127, No. 11474190, No. 11654002, and No. 11834010), the Program for Sanjin Scholars of Shanxi Province, Shanxi Scholarship Council of China, and the fund for Shanxi "1331 Project" Key Subjects Construction.

[1] H. J. Kimble, Nature (London) **453**, 1023 (2008).
[2] J. Simon, H. Tanji, S. Ghosh, and V. Vuletic, Nat. Phys. **3**, 765 (2007).
[3] H. B. Wu, J. Gea-Banacloche, and M. Xiao, Phys. Rev. Lett. **100**, 173602 (2008).
[4] A. M. Marino, R. C. Pooser, V. Boyer, and P. D. Lett, Nature (London) **457**, 859 (2009).
[5] Z. Z. Qin, L. M. Cao, H. L. Wang, A. M. Marino, W. P. Zhang, and J. T. Jing, Phys. Rev. Lett. **113**, 023602 (2014).
[6] K. C. Cox, G. P. Greve, J. M. Weiner, and J. K. Thompson, Phys. Rev. Lett. **116**, 093602 (2016).
[7] Z. H. Yan and X. J. Jia, Quantum Sci. Technol. **2**, 024003 (2017).

[8] G. Colangelo, F. M. Ciurana, L. C. Bianchet, R. J. Sewell, and M. W. Mitchell, Nature (London) **543**, 525 (2017).

[9] M. Ebert, M. Kwon, T. G. Walker, and M. Saffman, Phys. Rev. Lett. **115**, 093601 (2015).

[10] H. P. Specht, C. Nolleke, A. Reiserer, M. Uphoff, E. Figueroa, S. Ritter, and G. Rempe, Nature (London) **473**, 190 (2011).

[11] J. Hofmann, M. Krug, N. Ortegel, L. Gérard, M. Weber, W. Rosenfeld, and H. Weinfurter, Science **337**, 72 (2012).

[12] A. Facon, E. K. Dietsche, D. Grosso, S. Haroche, J. M. Raimond, M. Brune, and S. Gleyzes, Nature (London) **535**, 262 (2016).

[13] A. Stute, B. Casabone, P. Schindler, T. Monz, P. O. Schmidt, B. Brandstätter, T. E. Northup, and R. Blatt, Nature (London) **485**, 482 (2012).

[14] D. Hucul, I. V. Inlek, G. Vittorini, C. Crocker, S. Debnath, S. M. Clark, and C. Monroe, Nat. Phys. **11**, 37 (2015).

[15] X. Zhang, K. Zhang, Y. C. Shen, S. N. Zhang, J. N. Zhang, M. H. Yung, J. Casanova, J. S. Pedernales, L. Lamata, E. Solano, and K. Kim, Nat. Commun. **9**, 195 (2018).

[16] E. Flurin, N. Roch, J. D. Pillet, F. Mallet, and B. Huard, Phys. Rev. Lett. **114**, 090503 (2015).

[17] A. Narla, S. Shankar, M. Hatridge, Z. Leghtas, K. M. Sliwa, E. Zalys-Geller, S. O. Mundhada, W. Pfaff, L. Frunzio, R. J. Schoelkopf, and M. H. Devoret, Phys. Rev. X **6**, 031036 (2016).

[18] V. Fiore, Y. Yang, M. C. Kuzyk, R. Barbour, L. Tian, and H. L. Wang, Phys. Rev. Lett. **107**, 133601 (2011).

[19] Q. Lin, J. Rosenberg, X. S. Jiang, K. J. Vahala, and O. Painter, Phys. Rev. Lett. **103**, 103601 (2009).

[20] R. Riedinger, S. Hong, R. A. Norte, J. A. Slater, J. Y. Shang, A. G. Krause, V. Anant, M. Aspelmeyer, and S. Groblacher, Nature (London) **530**, 313 (2016).

[21] R. W. Andrews, R. W. Peterson, T. P. Purdy, K. Cicak, R. W. Simmonds, C. A. Regal, and K. W. Lehnert, Nat. Phys. **10**, 321 (2014).

[22] Z. P. Liu, J. Zhang, Ş. K. Özdemir, B. Peng, H. Jing, X. Y. Lü, C. W. Li, L. Yang, F. Nori, and Y. X. Liu, Phys. Rev. Lett. **117**, 110802 (2016).

[23] S. Kiesewetter, R. Y. Teh, P. D. Drummond, and M. D. Reid, Phys. Rev. Lett. **119**, 023601 (2017).

[24] E. Saglamyurek, N. Sinclair, J. Jin, J. A. Slater, D. Oblak, F. Bussieres, M. George, R. Ricken, W. Sohler, and W. Tittel, Nature (London) **469**, 512 (2011).

[25] M. J. Zhong, M. P. Hedges, R. L. Ahlefeldt, J. G. Bartholomew, S. E. Beavan, S. M. Wittig, J. J. Longdell, and M. J. Sellars, Nature (London) **517**, 177 (2015).

[26] A. Delteil, Z. Sun, W. B. Gao, E. Togan, S. Faelt, and A. Imamoğlu, Nat. Phys. **12**, 218 (2016).

[27] F. Kong, C. Y. Ju, Y. Liu, C. Lei, M. Q. Wang, X. Kong, P. F. Wang, P. Huang, Z. K. Li, F. Z. Shi, L. Jiang, and J. F. Du, Phys. Rev. Lett. **117**, 060503 (2016).

[28] R. Stockill, M. J. Stanley, L. Huthmacher, E. Clarke, M. Hugues, A. J. Miller, C. Matthiesen, C. Le Gall, and M. Atatüre, Phys. Rev. Lett. **119**, 010503 (2017).

[29] S. L. Braunstein and P. van Loock, Rev. Mod. Phys. **77**, 513 (2005).

[30] J. W. Pan, Z. B. Chen, C. Y. Lu, H. Weinfurter, A. Zeilinger, and M. Żukowski, Rev. Mod. Phys. **84**, 777 (2012).

[31] M. R. Huo, J. L. Qin, J. L. Cheng, Z. H. Yan, Z. Z. Qin, X. L. Su, X. J. Jia, C. D. Xie, and K. C. Peng, Sci. Adv. **4**, eaas9401 (2018).

[32] Y. Y. Zhou, J. Yu, Z. H. Yan, X. J. Jia, J. Zhang, C. D. Xie, and K. C. Peng, Phys. Rev. Lett. **121**, 150502 (2018).

[33] Z. H. Yan, L. Wu, X. J. Jia, Y. H. Liu, R. J. Deng, S. J. Li, H. Wang, C. D. Xie, and K. C. Peng, Nat. Commun. **8**, 718 (2017).

[34] H. Vahlbruch, M. Mehmet, K. Danzmann, and R. Schnabel, Phys. Rev. Lett. **117**, 110801 (2016).

[35] X. H. Bao, A. Reingruber, P. Dietrich, J. Rui, A. Dück, T. Strassel, L. Li, N. L. Liu, B. Zhao, and J. W. Pan, Nat. Phys. **8**, 517 (2012).

[36] Z. H. Yan, Y. H. Liu, J. L. Yan, and X. J. Jia, Phys. Rev. A **97**, 013856 (2018).

[37] H. J. Briegel, W. Dür, J. I. Cirac, and P. Zoller, Phys. Rev. Lett. **81**, 5932 (1998).

[38] L. M. Duan, M. D. Lukin, J. I. Cirac, and P. Zoller, Nature (London) **414**, 413 (2001).

[39] K. S. Choi, H. Deng, J. Laurat, and H. J. Kimble, Nature (London) **452**, 67 (2008).

[40] H. Zhang, X. M. Jin, J. Yang, H. N. Dai, S. J. Yang, T. M. Zhao, J. Rui, Y. He, X. Jiang, F. Yang, G. S. Pan, Z. S. Yuan, Y. J. Deng, Z. B. Chen, X. H. Bao, S. Chen, B. Zhao, and J. W. Pan, Nat. Photon. **5**, 628 (2011).

[41] M. Hosseini, B. M. Sparkes, G. Campbell, P. K. Lam, and B. C. Buchler, Nat. Commun. **2**, 174 (2011).

[42] Y.-H. Chen, M.-J. Lee, I.-C. Wang, S. Du, Y.-F. Chen, Y.-C. Chen, and I. A. Yu, Phys. Rev. Lett. **110**, 083601 (2013).

[43] Y. O. Dudin, L. Li, and A. Kuzmich, Phys. Rev. A **87**, 031801(R) (2013).

[44] Y. F. Pu, N. Jiang, W. Chang, H. X. Yang, C. Li, and L. M. Duan, Nat. Commun. **8**, 15359 (2017).

[45] D. S. Ding, W. Zhang, Z. Y. Zhou, S. Shi, G. Y. Xiang, X. S. Wang, Y. K. Jiang, B. S. Shi, and G. C. Guo, Phys. Rev. Lett. **114**, 050502 (2015).

[46] P. Vernaz-Gris, K. Huang, M. T. Cao, A. S. Sheremet, and J. Laurat, Nat. Commun. **9**, 363 (2018).

[47] D. Deutsch, A. Ekert, R. Jozsa, C. Macchiavello, S. Popescu, and A. Sanpera, Phys. Rev. Lett. **77**, 2818 (1996).

[48] C. H. Bennett, G. Brassard, S. Popescu, B. Schumacher, J. A. Smolin, and W. K. Wootters, Phys. Rev. Lett. **76**, 722 (1996).

[49] B. Hage, A. Samblowski, J. Di-Guglielmo, A. Franzen, J. Fiurášek, and R. Schnabel, Nat. Phys. **4**, 915 (2008).

[50] R. Dong, M. Lassen, J. Heersink, C. Marquardt, R. Filip, G. Leuchs, and U. L. Andersen, Nat. Phys. **4**, 919 (2008).

[51] L. M. Duan, G. Giedke, J. I. Cirac, and P. Zoller, Phys. Rev. Lett. **84**, 4002 (2000).

[52] P. G. Kwiat, S. Barraza-Lopez, A. Stefanov, and N. Gisin, Nature (London) **409**, 1014 (2001).

[53] J. W. Pan, C. Simon, Č. Brukner, and A. Zeilinger, Nature (London) **410**, 1067 (2001).

[54] X. S. Ma, S. Zotter, J. Kofler, R. Ursin, T. Jennewein, Č. Brukner, and A. Zeilinger, Nat. Phys. **8**, 479 (2012).

[55] X. J. Jia, X. L. Su, Q. Pan, J. R. Gao, C. D. Xie, and K. C. Peng, Phys. Rev. Lett. **93**, 250503 (2004).

[56] J. Cviklinski, J. Ortalo, J. Laurat, A. Bramati, M. Pinard, and E. Giacobino, Phys. Rev. Lett. **101**, 133601 (2008).

[57] J. Appel, E. Figueroa, D. Korystov, M. Lobino, and A. I. Lvovsky, Phys. Rev. Lett. **100**, 093602 (2008).

[58] K. Honda, D. Akamatsu, M. Arikawa, Y. Yokoi, K. Akiba, S. Nagatsuka, T. Tanimura, A. Furusawa, and M. Kozuma, Phys. Rev. Lett. **100**, 093601 (2008).

[59] K. Jensen, W. Wasilewski, H. Krauter, T. Fernholz, B. M. Nielsen, M. Owari, M. B. Plenio, A. Serafini, M. M. Wolf, and E. S. Polzik, Nat. Phys. **7**, 13 (2010).

[60] A. Ourjoumtsev, A. Dantan, R. Tualle-Brouri, and P. Grangier, Phys. Rev. Lett. **98**, 030502 (2007).

[61] H. Takahashi, J. S. Neergaard-Nielsen, M. Takeuchi, M. Takeoka, K. Hayasaka, A. Furusawa, and M. Sasaki, Nat. Photon. **4**, 178 (2010).

[62] N. Sangouard, C. Simon, H. D. Riedmatten, and N. Gisin, Rev. Mod. Phys. **83**, 33 (2011).

[63] S. D. Barrett, P. P. Rohde, and T. M. Stace, New J. Phys. **12**, 093032 (2010).

[64] R. Reichle, D. Leibfried, E. Knill, J. Britton, R. B. Blakestad, J. D. Jost, C. Langer, R. Ozeri, S. Seidelin, and D. J. Wineland, Nature (London) **443**, 838 (2006).

[65] N. Kalb, A. A. Reiserer, P. C. Humphreys, J. J. W. Bakermans, S. J. Kamerling, N. H. Nickerson, S. C. Benjamin, D. J. Twitchen, M. Markham, and R. Hanson, Science **356**, 928 (2017).

[66] A. Datta, L. J. Zhang, J. Nunn, N. K. Langford, A. Feito, M. B. Plenio, and I. A. Walmsley, Phys. Rev. Lett. **108**, 060502 (2012).

[67] D. E. Browne, J. Eisert, S. Scheel, and M. B. Plenio, Phys. Rev. A **67**, 062320 (2003).

[68] L. M. Duan, G. Giedke, J. I. Cirac, and P. Zoller, Phys. Rev. Lett. **84**, 2722 (2000).

[69] R. Simon, Phys. Rev. Lett. **84**, 2726 (2000).

[70] J. Fiurášek, P. Marek, R. Filip, and R. Schnabel, Phys. Rev. A **75**, 050302(R) (2007).

[71] A. S. Coelho, F. A. S. Barbosa, K. N. Cassemiro, A. S. Villar, M. Martinelli, and P. Nussenzveig, Science **326**, 823 (2009).

[72] S. Muhammad, A. Tavakoli, M. Kurant, M. Pawłowski, M. Żukowski, and M. Bourennane, Phys. Rev. X **4**, 021047 (2014).

[73] Z. Y. Ou, Phys. Rev. A **78**, 023819 (2008).

[74] Y. S. Han, X. Wen, J. He, B. D. Yang, Y. H. Wang, and J. M. Wang, Opt. Express **24**, 2350 (2016).

[75] Y.-F. Hsiao, P.-J. Tsai, H.-S. Chen, S.-X. Lin, C.-C. Hung, C.-H. Lee, Y.-H. Chen, Y.-F. Chen, I. A. Yu, and Y.-C. Chen, Phys. Rev. Lett. **120**, 183602 (2018).

[76] J. Eisert, S. Scheel, and M. B. Plenio, Phys. Rev. Lett. **89**, 137903 (2002).